Bone 128 (2019) 115041

Contents lists available at ScienceDirect

Bone

journal homepage: www.elsevier.com/locate/bone

Full Length Article

The angiotensin converting enzyme 2/angiotensin-(1-7)/Mas Receptor axis as a key player in alveolar bone remodeling

Celso Martins Queiroz-Junior[a,*], Anna Clara Paiva Menezes Santos[a], Izabela Galvão[b], Giovanna Ribeiro Souto[c,d], Ricardo Alves Mesquita[d], Marcos Augusto Sá[a], Anderson José Ferreira[a,*]

[a] Translational Biology Lab, Department of Morphology, Institute of Biological Sciences, Universidade Federal de Minas Gerais, Brazil
[b] Immunopharmacology, Department of Biochemistry and Immunology, Institute of Biological Sciences, Universidade Federal de Minas Gerais, Brazil
[c] Department of Dentistry, Pontifical Chatholic University of Minas Gerais, Brazil
[d] Department of Oral Surgery and Pathology, School of Dentistry, Universidade Federal de Minas Gerais, Brazil

ARTICLE INFO

Keywords:
Renin-angiotensin system
Alveolar bone
Osteoblast
Osteoclast

ABSTRACT

The renin-angiotensin system (RAS), aside its classical hormonal properties, has been implicated in the pathogenesis of inflammatory disorders. The angiotensin converting enzyme 2/angiotensin-(1-7)/Mas Receptor (ACE2/Ang-(1-7)/MasR) axis owns anti-inflammatory properties and was recently associated with bone remodeling in osteoporosis. Thus, the aim of this study was to characterize the presence and effects of the ACE2/Ang-(1-7)/MasR axis in osteoblasts and osteoclasts *in vitro* and *in vivo*. ACE2 and MasR were detected by qPCR and western blotting in primary osteoblast and osteoclast cell cultures. Cells were incubated with different concentrations of Ang-(1-7), diminazene aceturate (DIZE – an ACE2 activator), A-779 (MasR antagonist) and/or LPS in order to evaluate osteoblast alkaline phosphatase and mineralized matrix, osteoclast differentiation and cytokine expression, and mRNA levels of osteoblasts and osteoclasts markers. An experimental model of alveolar bone resorption triggered by dysbiosis in rats was used to evaluate bone remodeling *in vivo*. Rats were treated with Ang-(1-7), DIZE and/or A-779 and periodontal samples were collected for immunohistochemistry, morphometric analysis, osteoblast and osteoclast count and cytokine evaluation. Human gingival samples from healthy and periodontitis patients were also evaluated for detection of ACE2 and MasR expression. Osteoblasts and osteoclasts expressed ACE2 and MasR *in vitro* and *in vivo*. LPS stimulation or alveolar bone loss induction reduced ACE2 expression. Treatment of bone cells with Ang-(1-7) or DIZE stimulated osteoblast ALP, matrix synthesis, upregulated osterix, osteocalcin and collagen type 1 transcription, reduced IL-6 expression, and decreased osteoclast differentiation, RANK and IL-1β mRNA transcripts, and IL-6 and IL-1β levels, in a MasR-dependent manner. *In vivo*, Ang-(1-7) and DIZE decreased alveolar bone loss through improvement of osteoblast/osteoclast ratio. A-779 reversed such phenotype. ACE2/Ang-(1-7)/MasR axis activation reduced IL-6 expression, but not IL-1β. ACE2 and MasR were also detected in human gingival samples, with higher expression in the healthy than in the inflamed tissues. These findings show that the ACE2/Ang-(1-7)/MasR is an active player in alveolar bone remodeling.

1. Introduction

The renin-angiotensin system (RAS) is a hormonal cascade long known for controlling cardiovascular and renal physiology and disease [1]. The classical vasoconstrictive actions of the Angiotensin-Converting Enzyme (ACE)/Angiotensin (Ang) II/AT_1 Receptor (AT_1R) axis are counterbalanced by the ACE2/Ang-(1-7)/Mas Receptor (MasR) axis and also by recently described RAS members, including Alamandine and its Mas-related G-coupled receptor type D (MrgDR) [2]. Additionally, significant evidence from the last decades reveals that RAS functions go far beyond blood pressure control [3].

Remarkable experimental and also some clinical data implicate RAS components as active inflammatory mediators. Several studies demonstrate that AT_1R activation by Ang II induces leukocyte migration, release of pro-inflammatory cytokines (IL-1β, IL-6, TNF, CXCL-1 and others), fibrosis and NFκB activation in different contexts, such as

* Corresponding authors at: Av. Pres. Antônio Carlos, 6627, Pampulha, MG 31270-901, Brazil.
E-mail addresses: cmqj@yahoo.com.br, cmqj@ufmg.br (C.M. Queiroz-Junior), anderson@icb.ufmg.br (A.J. Ferreira).

https://doi.org/10.1016/j.bone.2019.115041
Received 14 February 2019; Received in revised form 15 August 2019; Accepted 19 August 2019
Available online 20 August 2019

arthritis [4], lung fibrosis [5], diabetes [6] and acute nephropathy [7]. On the other hand, increasing body of evidence point that the ACE2/Ang-(1-7)/MasR axis owns anti-inflammatory properties. Ang-(1-7) reduces hypernociception, edema, fibrosis, TNF and IL-1β expression and tissue damage in inflammatory scenarios [8–11]. Indeed, MasR activation favors resolution of inflammation by inducing neutrophil apoptosis and efferocytosis [12]. Accordingly, RAS components have also been characterized as bone-remodeling-associated mediators.

Indeed, blocking Ang II actions with an AT_1R antagonist prevents bone loss associated to estrogen deficiency [13,14] and also bone remodeling triggered by strain [15]. Such events derived from increased rates of osteoblast and decreased osteoclast markers [15]. Similarly, inhibiting Ang II engagement to AT_1R treated inflammatory alveolar bone resorption induced by dysbiosis. In this scenario, losartan reduced inflammatory cytokines and osteoclast differentiation *in vivo* and *in vitro* [16]. In contrast to these data, characterization of the ACE2/Ang-(1-7)/MasR axis in bone metabolism is scarce. There is evidence that Ang-(1-7) improves structural and mineral bone lesions in ovariectomy-induced osteoporosis in rats [17,18] and decreases osteolytic damage in an intra-tibial tumor model [19].

Nevertheless, the expression of ACE2 and MasR by bone cells and their effects on bone remodeling triggered by dysbiosis and inflammation are not known. Therefore, the aim of this study was to characterize the role of the ACE2/Ang-(1-7)/MasR axis in alveolar bone resorption *in vitro* and *in vivo*.

2. Methods

2.1. Animals

Male Wistar rats weighing 250–300 g were obtained from the Animal House of the Biological Sciences Institute, Federal University of Minas Gerais (UFMG), Brazil. The rats were kept under light/dark cycle of 12/12 h at 23–25 °C with free access to water and food. For *in vitro* experiments, neonatal Wistar rats (4 d of age) were used for the extraction of calvaria osteoblasts and Wistar rats at 4 weeks for bone marrow extraction and osteoclast differentiation. All the experimental procedures were approved by the Committee on Ethics in the use of Animals of UFMG.

2.2. Primary osteoblast cell culture

Osteoblasts were extracted from the calvaria of neonatal Wistar rats (4 d old) following a classical published protocol [20]. Briefly, after euthanasia, calvaria were dissected, digested with 1 mg/ml collagenase type II (Gibco) diluted in 0.25% trypsin at 37 °C and the obtained cells were cultured. The culture medium [minimal essential medium (α-MEM)(Gibco)] was supplemented with 10% fetal bovine serum (FBS; Gibco), 100 μg/ml gentamicin, 5 μg/ml ascorbic acid (Sigma-Aldrich, USA), and 2.16 mg/ml β-glycerophosphate (Sigma-Aldrich) (osteogenic medium) and was changed every 2 d during 7 d. Afterwards, the cells were counted and plated onto 24-well culture plates at a density of 1×10^4 cells/well or onto 96-well culture plates at a density of 2×10^3 cells/well. Then, 48 h after plating the osteoblasts, different concentrations of Ang-(1-7) (10^{-8}–10^{-6} M; Bachem) or DIZE, an ACE2 activator (10^{-5}–10^{-3} M; 6 h before LPS; diminazene aceturate; Sigma-Aldrich) with and without *E. coli* LPS (50 ng/ml; Sigma-Aldrich) and/or A-779 [10^{-5} M; 30 min before Ang-(1-7) or DIZE; Bachem] were added. Alkaline phosphatase and alizarin red assays were performed 14 d after cell stimulation. The experiments were conducted in quadruplicates for 96-well plates and triplicates for 24-well plate experiments. The groups used were: (1) Vehicle, which received only medium; (2) Ang-(1-7); (3) DIZE; (4) LPS; (5) LPS + Ang-(1-7); (6) LPS + DIZE; (7) A-779; (8) A-779 + Ang-(1-7) at 10^{-7} M of Ang-(1-7); (9) A-779 + DIZE at 10^{-5} M of DIZE; (10) A-779 + LPS; (11) A-779 + LPS + Ang-(1-7); (12) A-779 + LPS + DIZE.

2.2.1. Alkaline phosphatase assay

The alkaline phosphatase osteoblast activity was evaluated using the NBT/BCIP (nitro-blue tetrazolium/5-bromo-4-chloro-3-indolylphosphate) assay [21]. Fourteen days after osteoblast stimulation, the wells were washed with PBS and the NBT/BCIP (Invitrogen) [1(NBT):1(BCIP):8(PBS)] solution was added. The plates were incubated at 37 °C for 2 h. Thereafter, a solution of 10% SDS (Sigma) and 0.3% HCl in deionized water was added and the plates were incubated again at 37 °C overnight. The next day, the optical density of the supernatant was read in a spectrophotometer at 595 nm.

2.2.2. Alizarin red assay

Evaluation of osteoblast mineralized matrix synthesis was conducted using the alizarin red assay [22]. This assay was performed on 24-well plates with coverslips for cell culture. Fourteen days after cell stimulation, the wells were washed with PBS, fixed with 4% glutaraldehyde in PBS for 15 min and washed again. Alizarin red solution (40 mM, pH 4.2) was added to the wells and the plate was shaken for 20 min. The dye was removed, the wells were washed with distilled water and the coverslips were mounted on slides, which were photographed for analysis. Five fields (4× magnification; totalizing ~17 mm^2) were photographed in each coverslip for analysis. The area with mineralized matrix was quantified using the ImageJ software. Experiments were repeated at least twice.

2.3. Osteoclast cell culture

Cells extracted from the bone marrow of the tibia and femur of 4 week-old male Wistar rats were incubated in D-MEM (Cultilab) medium supplemented with 10% fetal bovine serum and with soluble macrophage colony-stimulating factor (M-CSF; 100 ng/ml; Peprotech) for 10 d to generate pre-osteoclasts (macrophages). Then, the cells were counted and plated in 24-well culture plates at a density of 1×10^4 cells/well or in 96-well culture plates at a density of 1×10^3 cells/well. Soluble receptor activator of nuclear factor-kB ligand (RANKL; 100 ng/ml; Peprotech) was added to the cells to stimulate the differentiation of macrophages into osteoclasts. This conditioned culture medium was changed every 2 d, for 3 times. Then Ang-(1-7), DIZE, LPS and/or A-779 were added to stimulate the cells, using the same protocol described in the osteoblast experiments.

2.3.1. TRAP assay

Ten days after osteoclast stimulation, TRAP staining was performed with the acid phosphatase leukocyte (TRAP) Kit (Sigma-Aldrich), following manufacturer's recommendations. The whole wells were photographed (20× magnification) for counting the multinucleated (two or more nuclei) TRAP-positive cells. Experiments were repeated at least twice.

2.4. MTT cell viability assay

Osteoblast and osteoclast cell viability was detected with the MTT assay [20]. Thirty-six hours after the cell stimulation with Ang-(1-7), DIZE, LPS and/or A-779, the wells were washed with PBS and a solution of MTT (1 mg/ml) in α-MEM or D-MEM was added to the cells, which were maintained in the CO_2 incubator for 4 h at 37 °C. After incubation, another wash was done with PBS. Then, a solution of isopropanol/HCl was added and the samples were shaken to promote the elution of the formazan crystals. The supernatant was quantified by measuring the absorbance values at 595 nm in a spectrophotometer.

2.5 Quantitative. real-time PCR

Total RNA was isolated from the osteoblast and osteoclast cultures 2, 7 and/or 14 d after cell stimulation using Trizol reagent (Thermo Fisher Scientific, Grand Island, NY, USA) according to the

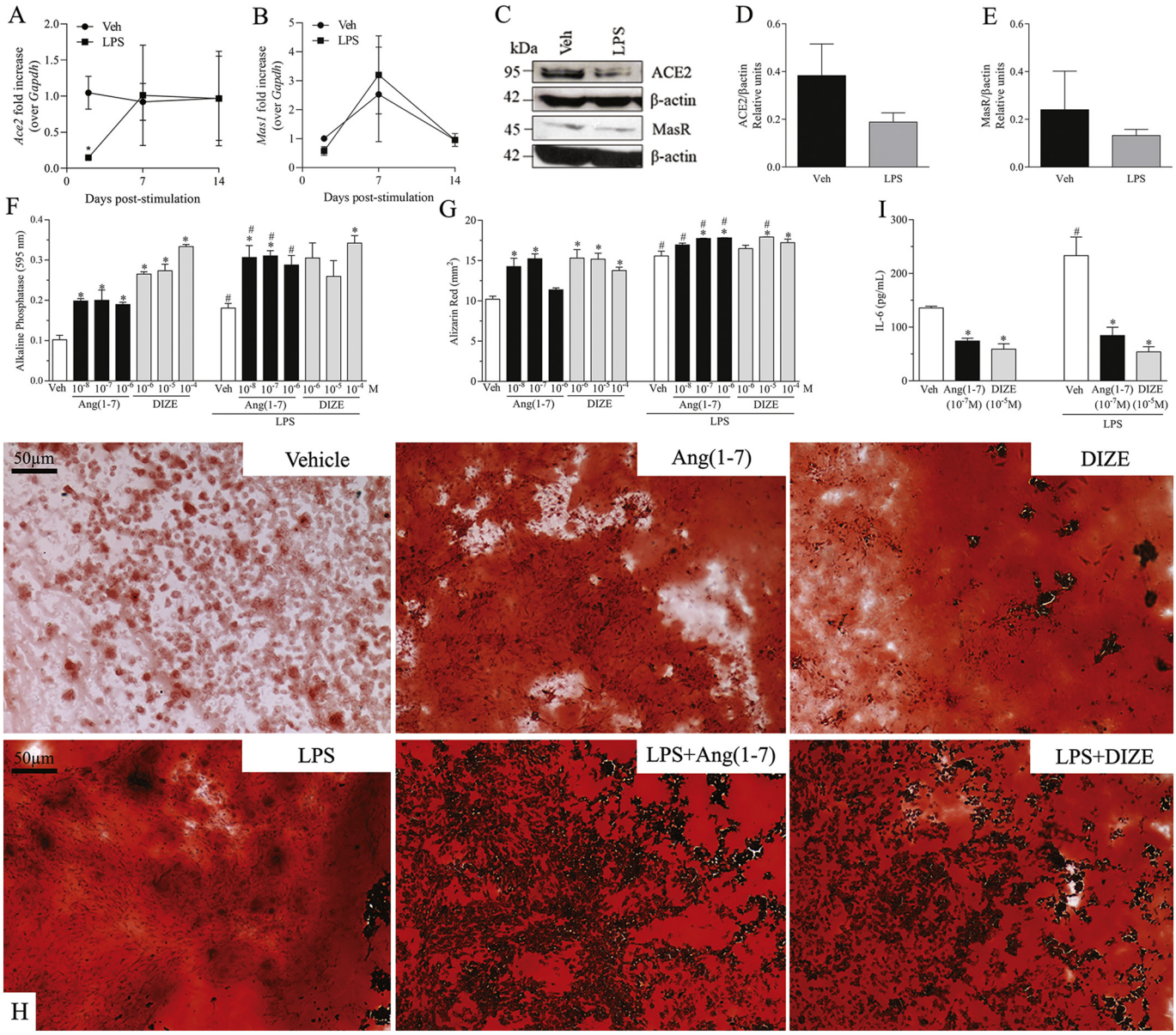

Fig. 1. The ACE2/Ang-(1-7)/MasR axis in primary osteoblasts. (A) ACE2 and (B) MasR mRNA were detected in osteoblasts by qPCR 2, 7 and 14 d post-LPS stimulation. (C) Representative western blots for ACE2 and MasR, which were analyzed by densitometry using the ImageJ software [ratio of ACE2 (D) or MasR (E) and the control β-actin] 2 d post-stimulation. (F) Alkaline phosphatase activity was detected colorimetrically 14 d after cell stimulation. (G) Alizarin red quantification was conducted morphometrically 14 d after LPS stimulation. (H) Representative images of alizarin red stained osteoblast samples. (I) IL-6 was detected by ELISA in osteoblast supernatants 24 h post-stimulation. * $p < 0.05$ *versus* Vehicle. $^{\#}$ $p < 0.05$ *versus* the respective group without LPS. Statistical evaluation was performed using Student's *t*-test for comparison of two independent groups and one-way ANOVA followed by the Newman-Keuls post-test for more than two groups.

Table 1
Effects of Ang-(1-7) and DIZE on osteoblast and osteoclast markers in the absence or presence of LPS.

		Vehicle	Ang-(1-7) 10^{-7} M	DIZE 10^{-5} M	LPS	LPS + Ang-(1-7) 10^{-7} M	LPS + DIZE 10^{-5} M
Osteoblasts	Runx2	1,00 ± 0,07	0,97 ± 0,27	1,98 ± 0,81	1,42 ± 0,26	1,63 ± 0,29	2,08 ± 0,67
	Osterix	1,37 ± 0,52	1,39 ± 0,24	1,44 ± 0,34	1,61 ± 0,12	2,43 ± 0,30$^{*,\#}$	1,79 ± 0,21
	Osteocalcin	1,89 ± 0,87	2,62 ± 0,45	2,56 ± 0,90	0,71 ± 0,29	1,84 ± 0,96	0,42 ± 0,13
	Collagen type 1	0,71 ± 0,20	2,55 ± 0,46*	3,32 ± 1,56	4,97 ± 1,92$^{\#}$	6,44 ± 1,48$^{\#}$	4,67 ± 1,98
Osteoclasts	Interleukin-1β	1,15 ± 0,34	3,19 ± 1,76	3,4 ± 0,35	31,26 ± 3,04$^{\#}$	5,21 ± 0,55*	20,36 ± 5,96$^{\#}$
	Metalloproteinase-13	4,74 ± 3,78	2,18 ± 1,17	2,87 ± 0,80	22,92 ± 5,06$^{\#}$	6,79 ± 3,66	9,95 ± 5,95
	Rank	1,60 ± 0,85	1,82 ± 0,95	2,3 ± 1,25	5,78 ± 0,5$^{\#}$	3,64 ± 0,35*	4,99 ± 0,40

* $p < 0.05$ *versus* Vehicle or LPS.
$^{\#}$ $p < 0.05$ *versus* the respective group without LPS; One-way ANOVA followed by Newman-Keuls.

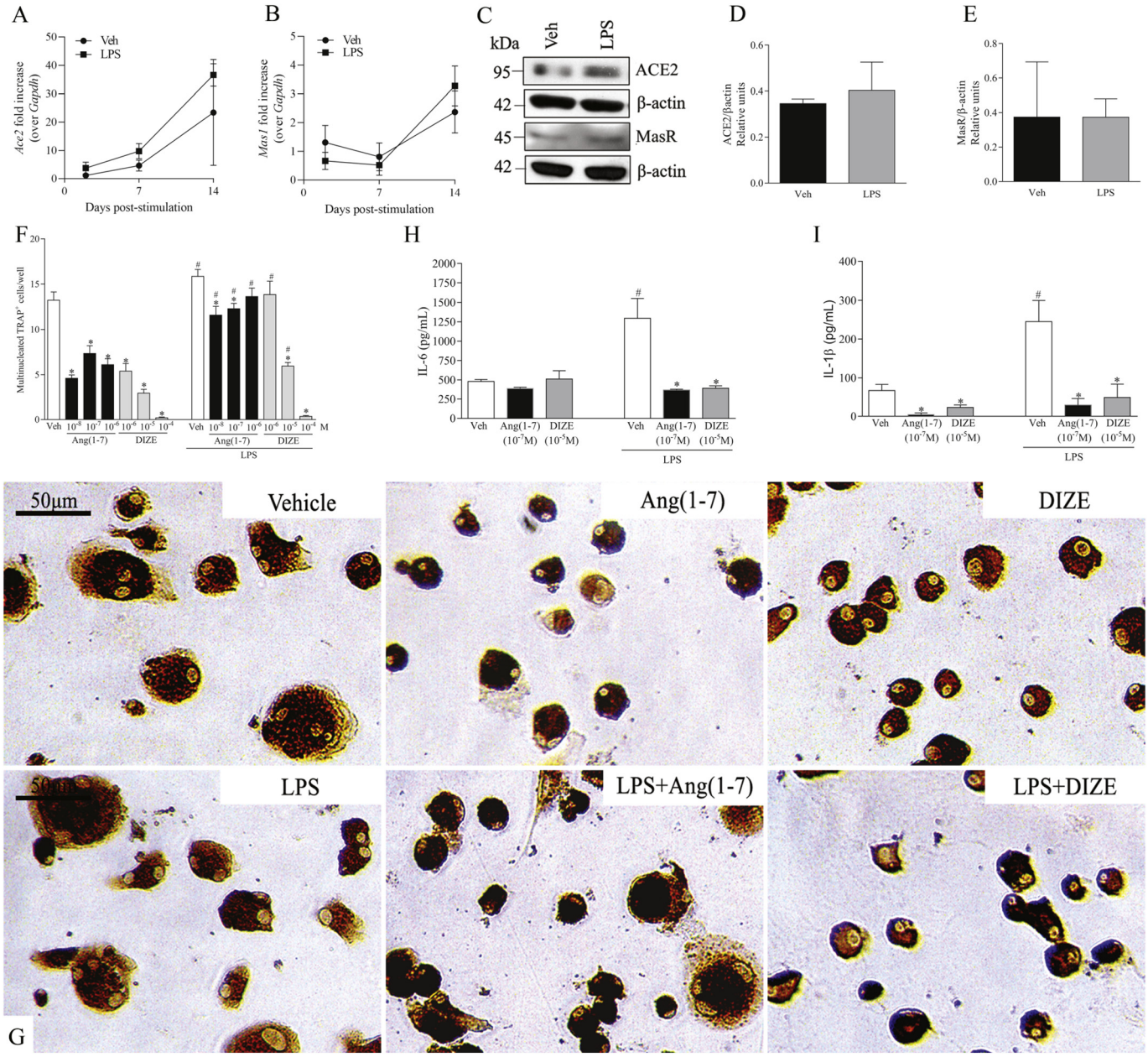

Fig. 2. The ACE2/Ang-(1-7)/MasR axis in bone marrow-derived osteoclasts. (A) ACE2 and (B) MasR mRNA were detected in osteoclasts by qPCR 2, 7 and 14 d after stimulation with LPS. (C) Representative western blots for ACE2 and MasR, which were analyzed by densitometry using the ImageJ software [ratio of ACE2 (D) or MasR (E) and the control β-actin] 48 h post-stimulation. (F) Quantification of TRAP-positive multinucleated cells 10 d after cell stimulation. (G) Representative photomicrographs from osteoclast cell culture. (H) IL-6 and (I) IL-1β were quantified by ELISA in cell culture supernatants 24 h post-stimulation. * $p < 0.05$ *versus* Vehicle; # $p < 0.05$ *versus* the respective group without LPS. Statistical analysis was performed using Student's *t*-test for comparison of two independent groups and one-way ANOVA followed by the Newman-Keuls post-test for more than two groups.

manufacturer's recommendations. Real-time PCR quantitative mRNA analyses were performed on a 7500 Fast Real-Time PCR system using iTaq Universal SYBR green supermix (Bio-Rad, Hercules, CA, USA) after reverse transcription reactions of 1 μg RNA utilizing RevertAid First Strand cDNA Synthesis kit (Thermo Scientific). Relative expression of MasR (primers: forward - 5′TTG GTG GTG AAG ATA CGG AAG 3′ and reverse - 5′ ATG GTG GAG AAA AGC AAG GA 3′), ACE2 (primers: forward - 5′ TCC TTC TCA GCC TTG TTG CT 3′ and reverse - 5′ CAG CCT CGT TCA TCT TTT GG 3′), Osterix (primers: forward - 5′ TGA GCT GGA ACG TCA CGT GC 3′ and reverse - 5′ AAG AGG AGG CCA GCC AGA CA 3′), Runt-related transcription factor 2 (RUNX2, primers: forward - 5′ GCC ACC ACT CAC TAC CAC AC 3′ and reverse - 5′ CAG CGT CAA CAC CAT CAT TC 3′), Osteocalcin (primers: forward – 5′ GGA CCA TCT TTC TGC TCA CTC TG 3′ and reverse - 5 GTT CAC TAC CTT ATT GCC CTC CTG 3′), Collagen 1A (primers: forward - 5′ TAG GAG TCG AGG GAC CCA AG 3′ and reverse - 5′ AGG CTC TCC CTT AGG ACC AG 3′), RANK (primers: forward - 5′ AAC TCC AAC TCA ACG GAT GG 3′ and reverse - 5′ TGG GAA GGC CTA TGC TGT AG 3′), IL-1β (primers: forward - 5′ TGC TGT CTG ACC CAT GTG AG 3′ and reverse - 5′ CCA AGG CCA CAG GGA TTT TG 3′) or Metalloproteinase-13 (MMP-13, primers: forward – 5′ CCC TGG AGC CCT GAT GTT 3′ and reverse – 5′ TGG GTC ACA CTT CTC TGG TG 3′) was determined by the comparative threshold cycle method using $2^{-\Delta\Delta ct}$ normalized with GAPDH constitutive gene (primers: forward - 5′-ACG GCC GCA TCT TCT TGT GCA-3′ and reverse - 5′-CGG CCA AAT CCG TTC ACA CCG A-3′) and expressed as fold change compared with control.

Table 2
Effects of A779 on osteoblasts and osteoclasts in the absence or presence of LPS.

	Vehicle	A-779	Ang-(1-7) 10^{-7} M	Ang-(1-7) + A-779	DIZE 10^{-5} M	DIZE + A-779
Alkaline phosphatase (AU)	0,13 ± 0,003	0,0845 ± 0,005	0,23 ± 0,013*	0,113 ± 0,007&	0,192 ± 0,009*	0,117 ± 0,023&
Alizarin red (mm^2)	8,131 ± 0,336	8,894 ± 0,125	14,59 ± 0,841*	9,895 ± 1,649*,&	15,02 ± 0,24*	8,135 ± 0,697*,&
TRAP (cells/well)	35,3 ± 0,903	34,3 ± 0,723	27,15 ± 0,613*	33,35 ± 0,805&	24,45 ± 1,132*	30,3 ± 0,412*,&

	LPS	LPS + A-779	LPS + Ang-(1-7) 10^{-7} M	LPS + Ang-(1-7) + A-779	LPS + DIZE 10^{-5} M	LPS + DIZE + A-779
Alkaline phosphatase (AU)	0,192 ± 0,019#	0,164 ± 0,010#	0,259 ± 0,009*	0,152 ± 0,005*,&	0,253 ± 0,003*,#	0,126 ± 0,003*,&
Alizarin red (mm^2)	13,31 ± 0,716#	11,02 ± 0,985	16,26 ± 0,412*	9,821 ± 1,239&	16,55 ± 0,258*,#	10,35 ± 1,056*,&
TRAP (cells/well)	53,6 ± 0,627#	52,15 ± 0,531#	46 ± 0,678*,#	52,75 ± 0,741#,&	42,1 ± 0,591*,#	50,5 ± 0,776*,#,&

Osteoblasts were cultivated for 14 d and osteoclasts for 10 d post-LPS stimulation. * $p < 0.05$ *versus* Vehicle or LPS; # $p < 0.05$ *versus* the respective group without LPS; & $p < 0.05$ *versus* the respective groups without A-779; one-way ANOVA followed by Newman-Keuls.

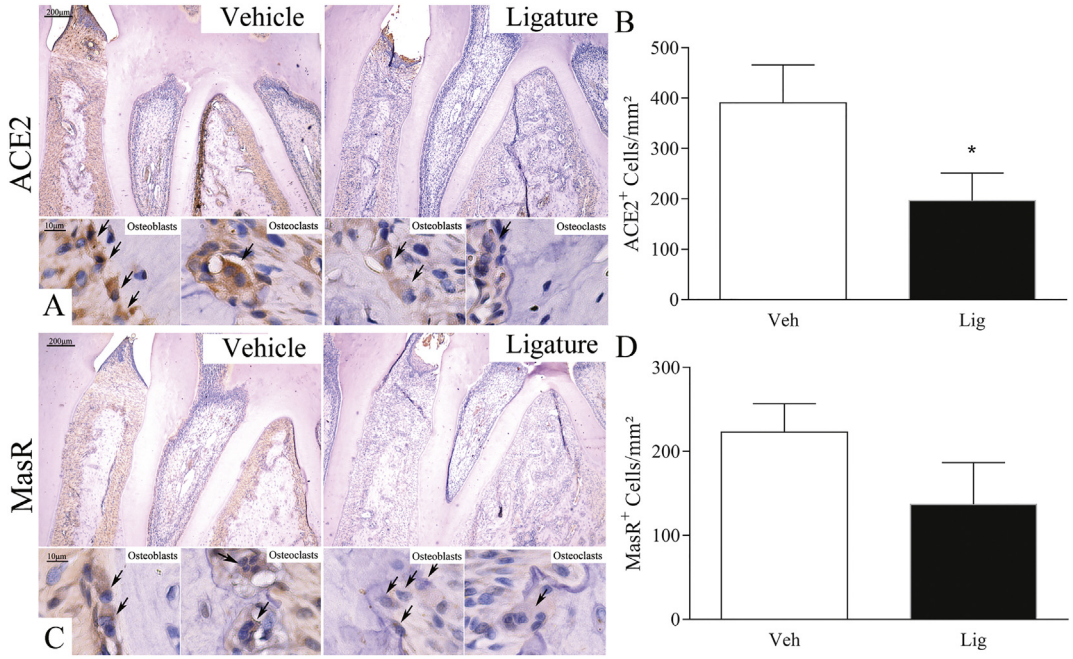

Fig. 3. The ACE2/Ang-(1-7)/MasR axis in periodontal tissues. Immunohistochemistry was performed to detect ACE2 (A) and MasR (C) in control ($n = 6$) and diseased (n = 6) samples. Total ACE2 (B) and MasR (D) immunostained cells were counted morphometrically. Arrows indicate osteoblasts and osteoclasts. * $p < 0.05$ *versus* Vehicle using unpaired Student's *t*-test.

2.6. Western blotting

Cell extract was obtained from osteoblast and osteoclast cultures 48 h after stimulation using Cell Lysis Buffer (1% Triton X100, 0.2 mM EDTA, 100 mM Tris/HCl, 20% Glicerol) with anti-proteases. Protein amounts were quantified with the Bradford assay reagent (Bio-Rad, CA, USA). Extracts (50 μg) were separated by electrophoresis on a denaturing 8–10% polyacrylamide-SDS gel and electrotransferred to nitrocellulose membranes. Membranes were incubated with specific primary antibodies [anti-MasR (Alomone) and anti-ACE2 (GeneTex)] overnight. Membranes were then incubated with the HPR-conjugated secondary antibody for 1 h at room temperature. Immunoreactive bands were visualized using western ECL substrate kit as indicated by the manufacturer (Bio-Rad, Hercules, CA, USA). For loading control, membranes were reprobed with anti-β-actin antibody (Sigma).

2.7. ACE2 activity

Evaluation of ACE2 activity was performed using osteoblasts and osteoclasts following previously described methods [25]. Cells were mechanically lysed in 1 M NaCl, 75 mM Tris-HCl, 1% DMSO and 0.5 μM $ZnCl_2$ solution, at pH 7.4. Fifty microliters of the cell extract or recombinant ACE2 (R&D systems, USA) were incubated with the ACE2 substrate [fluorogenic peptide VI, Mca-YVADAPK(Dnp)-OH, ES007, R&D Systems]. The enzymatic activity was measured with a Spectra Max Gemini EM Fluorescence Reader (Molecular Devices) every 5 min for 60 min immediately after addition of the substrate.

2.8. In vivo experimental model of alveolar bone resorption

Alveolar bone resorption was evaluated *in vivo* using a well-established experimental model of periodontal disease, as described previously [23,24]. Briefly, rats were anesthetized with ketamine and xylazine (80 and 9 mg/kg, i.m., respectively) and a sterile silk ligature was tied around the cervix of the second left upper molar tooth. The ligature remained around the tooth for 7 d. In the last day, the animals were euthanized and periodontal tissues were collected for evaluation.

2.8.1. Drug treatment

In vivo treatments comprised the following groups ($n = 5$–6 rats per

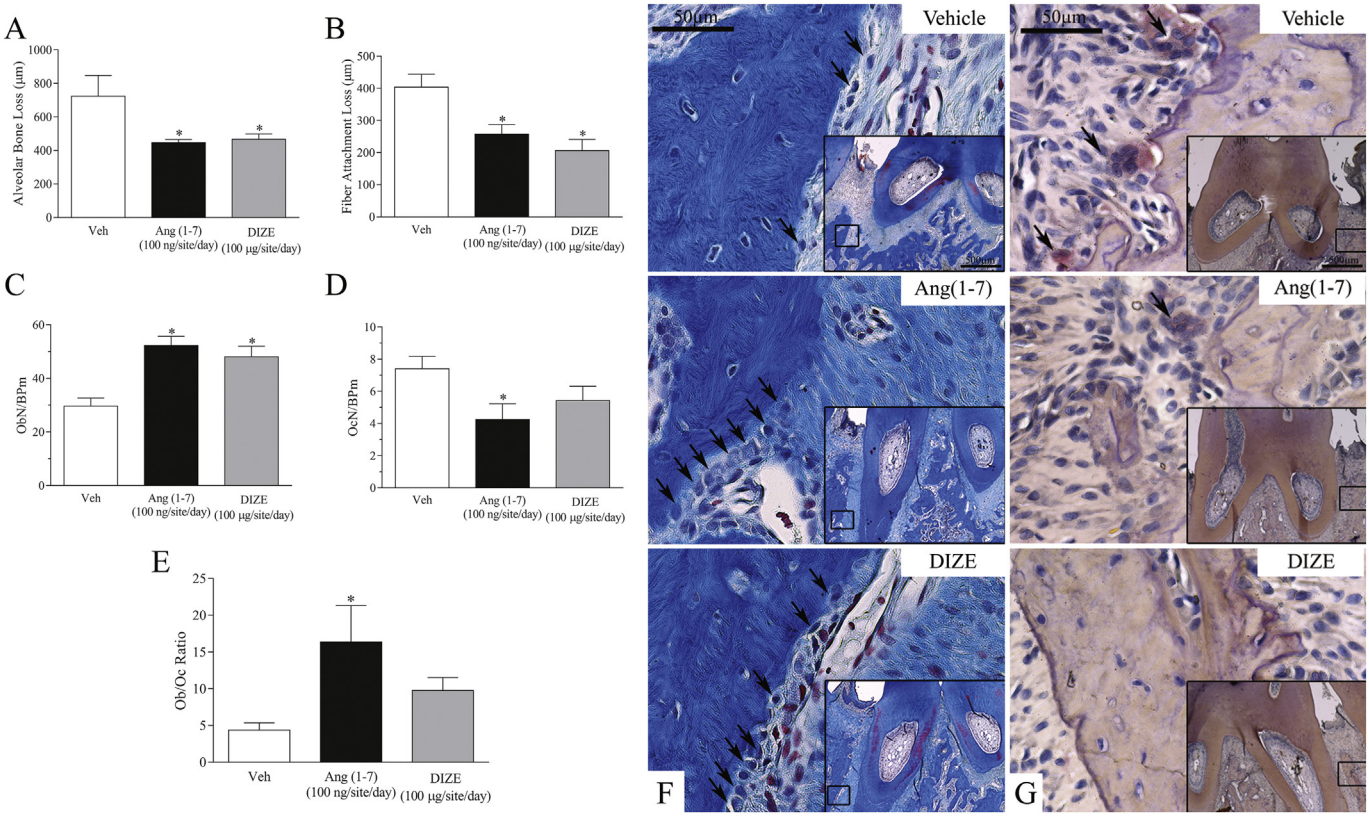

Fig. 4. Effects of Ang-(1-7) or DIZE on alveolar bone resorption. Quantification of (A) alveolar bone loss and (B) fiber attachment loss were performed morphometrically using the ImageJ software. Counting of (C) osteoblast-like cells and (D) TRAP-positive cells next to the alveolar bone associated to the tooth with ligature. (E) Osteoblast/osteoclast ratio. Representative images of (F) Masson's trichrome stained osteoblast-like cells (arrows) and (G) TRAP-positive cells (arrows). $N = 5$ rats/group. * $p < 0.05$ *versus* Vehicle using one-way ANOVA followed by the Newman-Keuls post-test.

Table 3
Effects of A-779 in alveolar bone resorption *in vivo*.

	Vehicle	A-779	Ang-(1-7) 100 ng/site/day	Ang-(1-7) + A-779	DIZE 100 µg/site/day	DIZE + A-779
Alveolar bone loss (µm)	604,2 ± 75,59	525,2 ± 62,78	335,6 ± 69,68*	483,1 ± 72,6	440,6 ± 27,12*	554,4 ± 54,32
Fiber attachment loss (µm)	387,2 ± 24,89	349,7 ± 21,3	271,1 ± 32,01*	371 ± 8,46	257,4 ± 28,82*	410,6 ± 39,39
ObN/BPm	25,15 ± 4,6	37,49 ± 0,94	47,42 ± 7,9	31,66 ± 0,07	41,88 ± 2,59*	34,94 ± 3,49
OcN/BPm	7,405 ± 0,77	7,855 ± 0,59	3,549 ± 0,61*	7,944 ± 0,63#	5,427 ± 0,88	8,271 ± 2,19
Ob/Oc ratio	4,374 ± 0,98	5,239 ± 0,23	13,39 ± 0,25*	4,036 ± 0,31#	9,757 ± 1,78	4,558 ± 0,63

N = 5 rats/group. * $p < 0.05$ *versus* Vehicle; # $p < 0.05$ *versus* the respective group without A-779, one-way ANOVA followed by Newman Keuls.

group): (1) Vehicle, rats with ligature treated with vehicle; (2) Ang-(1-7), rats with ligature receiving Ang-(1-7) 100 ng/site/day; (3) DIZE, rats with ligature that received DIZE 100 µg/site/day; (4) A-779 + Ang-(1-7), rats with ligature receiving A-779 200 ng/site/day and Ang-(1-7) 100 ng/site/day; (5) A-779 + DIZE, rats with ligature that received A-779 200 ng/site/day and DIZE 100 µg/site/day. In order to perform the treatments, rats were anesthetized as described above and the drugs were injected (50 µl) locally into the gingival tissue close to the ligated tooth from the 1st to the 7th day after ligature placement.

2.8.2. Morphometric analysis

After the experimental period, maxillary samples were removed and processed for routine histological evaluation. The sample slices were stained with Masson's trichrome and photographed to determine the loss of alveolar bone and the fiber attachment. The distance from the cemento-enamel junction (CEJ) to the most coronal edge of the alveolar bone crest (ABC) was measured by the Image J software (National Institutes of Health, Bethesda, USA). Alveolar bone loss (µm) is reported as the difference between sites, compared to the control site (non-ligated molar) of the same animal. The loss of fiber attachment was quantified by measuring the distance between the CEJ and the most coronal fiber insertion using the ImageJ software. The samples were also evaluated for counting the number of osteoblasts next to the alveolar bone associated to the 2nd molar with ligature. Osteoblasts were identified in view of their position next to alveolar bone and their morphological characteristics (size and shape). The number of cells was expressed as osteoblasts/bone perimeter (ObN/BPm). Histological maxillary samples were also used for TRAP staining (following manufacture instructions; Sigma-Aldrich) and count of TRAP-positive osteoclasts. TRAP-positive cells located next to alveolar bone were counted and the results were expressed as osteoclasts/bone perimeter (OcN/BPm).

2.8.3. Immunohistochemistry

Histological maxillary slices were processed for immunohistochemistry (IHC). The IHC reaction was performed using the streptavidin-biotin protocol. Endogenous peroxidase blockade was performed with 0.3% hydrogen peroxide and antigenic recovery with

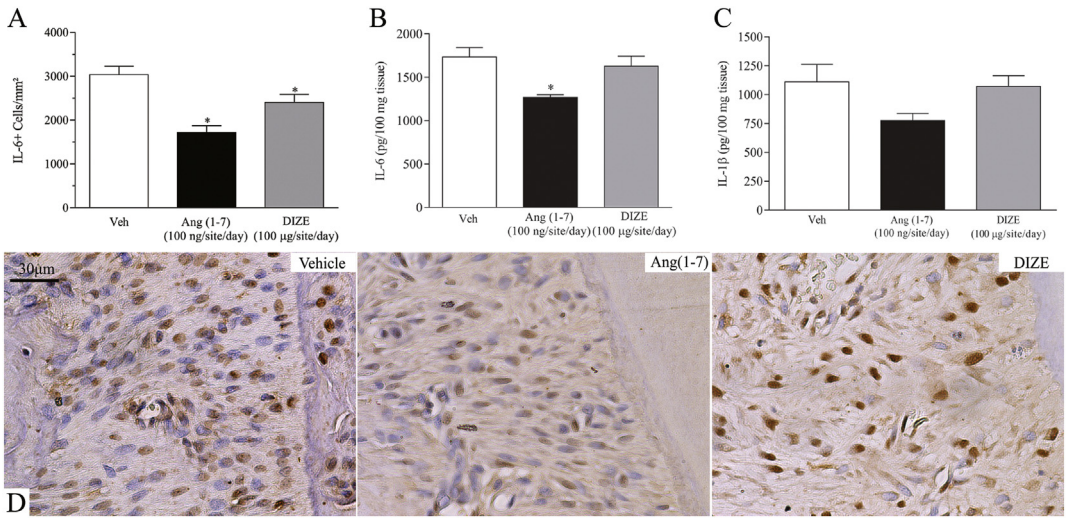

Fig. 5. Expression of cytokines in periodontal tissues after Ang-(1-7) or DIZE treatment. (A) Quantification of immunostained IL-6 cells by immunohistochemistry in periodontal tissues. (B) IL-6 and (C) IL-1β expression by ELISA in periodontal tissue homogenates. (D) Representative images of IL-6-immunostained cells. N = 5 rats/groups. * $p < 0.05$ *versus* Vehicle using one-way ANOVA followed by the Newman-Keuls post-test.

0.1 M citrate buffer solution. The samples were then incubated with the primary antibodies, *i.e.* anti-ACE2 (GeneTex) at a dilution of 1:400, anti-MasR (Alomone) at a dilution of 1:100, and anti-IL-6 (Imuny) at a dilution of 1:20. The reaction was revealed with DAB chromogenic solution and counterstained with hematoxylin. Negative reaction controls comprised samples in which the primary antibodies were omitted. Immuno-stained cells were counted in periodontal tissues and expressed as positive cells/mm^2.

2.9. ELISA

Cytokines associated to bone resorption were evaluated in *in vitro* and *in vivo* experiments using ELISA. For *in vitro* experimentation, 24 h post-stimulation, the cell supernatants were collected to analyze the levels of IL-6 and IL-1β using commercially available ELISA kits (R&D Systems). For *in vivo* experiments, maxillary samples were removed and processed with anti-proteases in order to evaluate the expression of the same cytokines. The results are expressed as picograms of cytokine per ml of supernatant or per 100 mg of tissues.

2.10. Human gingival samples

Six human gingival samples from 3 healthy and 3 periodontitis patients were obtained for qualitative evaluation of ACE2 and MasR expression. This study was approved by the Committee of Ethics in Research at UFMG, Brazil (423/11). Donor patients did not have systemic diseases or immunological abnormalities. Probing depth (PD), clinical attachment loss (CAL), bleeding on probing (BOP) and oral hygiene index were analyzed by a single trained examiner. Individuals with proximal CAL ≥ 3 mm in 2 or more non-adjacent teeth were diagnosed as patients with periodontitis (Tonetti and Claffey, 2005). Gingival samples from healthy patients were collected from the gingiva that overlapped the third molar at the time of extraction. The collected gingival samples were fixed in 10% buffered formalin, histologically processed, sectioned and submitted to immunohistochemistry for ACE2 and MasR, as described in Section 2.8.3.

2.11. Statistical analysis

Quantitative data were expressed as mean ± standard error of the mean. Differences between means were assessed by unpaired Student's *t*-test or one-way ANOVA followed by Newman-Keuls test. Differences with $p < 0.05$ were considered statistically significant.

3. Results

3.1. The ACE2/Ang-(1-7)/MasR axis in osteoblasts

In order to characterize the involvement of the ACE2/Ang-(1-7)/MasR axis on bone remodeling, we first evaluated the expression of ACE2 and MasR by osteoblasts at mRNA and protein levels. Primary osteoblasts expressed both the enzyme and receptor involved in the Ang-(1-7) formation and activity (Fig. 1A–E). Such expression slightly decreased after 2 d of LPS stimulation - significant reduction for ACE2 mRNA -, but returned to basal levels at 7 and 14 d post-stimulation (Fig. 1A–B).

Afterwards, we stimulated osteoblast cell cultures with different concentrations of Ang-(1-7) or DIZE, a compound already known to increase ACE2 activity [25] (Sup. Fig. 1A), and evaluated osteoblast enzyme activity and mineralized matrix synthesis. Both Ang-(1-7) and DIZE significantly increased osteoblast metabolism, which translated into higher ALP activity (Fig. 1F) and alizarin red-stained area (Fig. 1G–H). The bacterial virulence factor LPS markedly stimulated osteoblasts, and this phenotype was even more pronounced after the treatments for ACE2/Ang-(1-7)/MasR axis activation (Fig. 1F–H). Accordingly, Ang-(1-7) increased the mRNA levels of the osteoblast differentiation marker osterix ($p < 0.05$ in the presence of LPS) and the osteoblast activity markers osteocalcin ($p > 0.05$, 39% and 159% increase *versus* Vehicle and LPS, respectively) and collagen 1A ($p < 0.05$ in the absence of LPS). The effects of DIZE over these markers were milder ($p > 0.05$), although it enhanced RUNX2, osteocalcin and collagen 1A mRNA levels in 98%, 35% and 367%, respectively, in the absence of LPS (Table 1).

As the ACE2/Ang-(1-7)/MasR axis is known for its anti-inflammatory properties, we also investigated whether the observed osteoblast activation could be associated with IL-6, a cytokine produced by osteoblasts and directly related to bone resorption [26]. LPS stimulation significantly increased IL-6 expression in cell culture. Ang-(1-7) and DIZE reduced both non-stimulated and LPS-induced IL-6 release by osteoblasts *in vitro* (Fig. 1I). Of note, Ang-(1-7) and DIZE did not influence osteoblast viability (Sup. Fig. 2A).

3.2. The ACE2/Ang-(1-7)/MasR axis in osteoclasts

We also evaluated the involvement of the ACE2/Ang-(1-7)/MasR axis in osteoclast differentiation. Osteoclasts differentiated from bone marrow cells expressed both mRNA and protein for ACE2 and MasR.

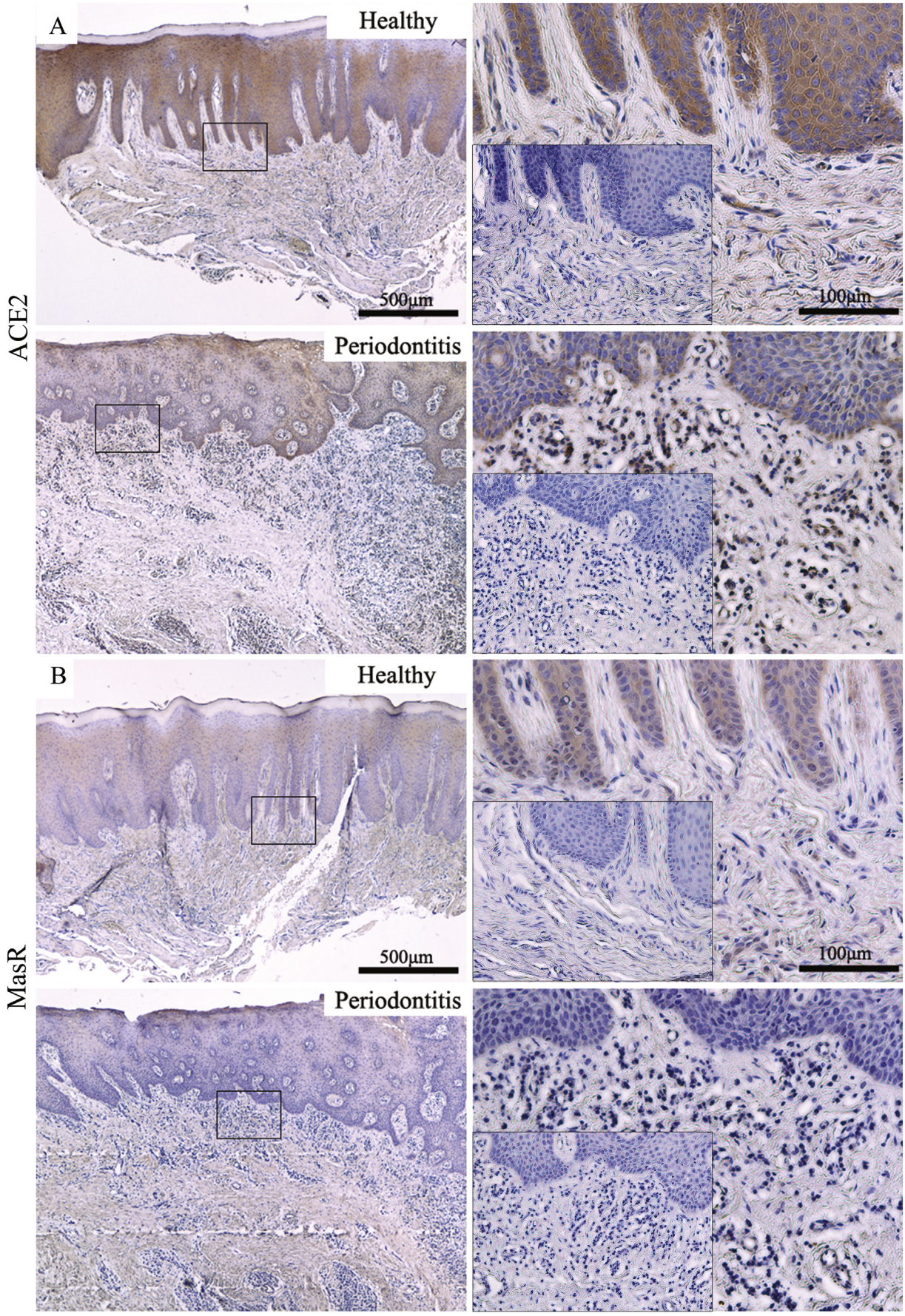

Fig. 6. The ACE2/Ang-(1-7)/MasR axis in human gingival tissues. Representative photomicrographs of (A) ACE2 and (B) MasR immunostained gingival samples obtained from healthy and periodontitis patients. The inserts indicate the respective IHC reaction controls.

The time-course expression presented increasing pattern and LPS stimulation did not interfere significantly with such profile (Fig. 2A–E).

The treatment of pre-osteoclasts with Ang-(1-7) or DIZE decreased osteoclast differentiation induced by RANKL. In the presence of LPS, this effect was less pronounced, given that only the 10^{-8} M and 10^{-7} M Ang-(1–7) and 10^{-5} M and 10^{-4} M DIZE concentrations reduced the formation of multinucleated TRAP-positive cells (Fig. 2F–G). It is worth noting that the 10^{-4} M DIZE concentration reduced cell viability (Sup. Fig. 2C). In line with these results, Ang-(1-7) reduced the mRNA levels of IL-1β ($p < 0.05$), MMP-13 ($p > 0.05$, 70% decrease *versus* LPS) and the receptor RANK ($p < 0.05$) in LPS-stimulated cells (Table 1). Similarly, DIZE also induced a decreased pattern of mRNA levels for these osteoclast differentiation and activity markers after LPS stimulation, but the differences were not statistically significant (Table 1).

Regarding inflammatory cytokines associated to bone resorption and synthesized by osteoclasts, LPS triggered increased IL-6 and IL-1β release in cell culture (Fig. 2H–I). Both Ang-(1-7) and DIZE prevented such higher expression in the presence of LPS, but in non-stimulated conditions, only reduced IL-1β (Fig. 2H–I).

3.3. The in vitro effects of Ang-(1-7) and DIZE are dependent on MasR activation

In order to investigate whether the afore mentioned effects of Ang-(1-7) and DIZE derived from MasR activation, we pre-treated cells with the MasR antagonist A-779 and evaluated the phenotype of osteoblasts and osteoclasts. In the presence of the antagonist, both ALP activity and mineralized matrix formation were not stimulated by the most effective concentrations of Ang-(1-7) or DIZE in primary osteoblast cultures (Table 2). Similarly, in osteoclast cultures, the protective effects triggered by ACE2/Ang-(1-7)/MasR axis activation on osteoclast differentiation were also prevented by A-779 (Table 2). These results indicate that the observed phenotypes were dependent on MasR activation.

3.4. The ACE2/Ang-(1-7)/MasR axis in ligature-induced alveolar bone resorption

We next evaluated the involvement of the ACE2/Ang-(1-7)/MasR axis in alveolar bone resorption *in vivo*. Different cell types, including fibroblasts, epithelium, endothelial cells, and also osteoblasts and osteoclasts, expressed ACE2 (Fig. 3A) and MasR (Fig. 3C) in periodontal tissues in physiological conditions. In contrast, such expression was weak in samples with alveolar bone loss associated to dysbiosis induced by the placement of a ligature around the 2nd molar (Fig. 3A–D). Noteworthy, the number of ACE2-positive cells significantly decreased in the bone resorptive context (Fig. 3B).

In another set of experiments, we locally treated ligature-rats with Ang-(1-7) or DIZE. Both ACE2/Ang-(1-7)/MasR axis activating therapies reduced bone resorption (Fig. 4A) and the related fiber attachment loss (Fig. 4B), which are hallmarks of periodontitis. Such phenotype associated to increased number of osteoblasts in bone edge (Fig. 4C and F) and reduced number of TRAP-positive osteoclasts (Fig. 4D and G). Accordingly, Ang-(1-7) significantly improved the osteoblast/osteoclast ratio (Fig. 4E). Indeed, all these effects were dependent on MasR, given that pre-treatment of rats with the MasR antagonist A-779 blocked all the beneficial effects of Ang-(1-7) and DIZE on alveolar bone and bone cells (Table 3).

In view of these results, we investigated whether Ang-(1-7) effects derived, at least in part, from its anti-inflammatory potential. Similarly to *in vitro* conditions, Ang-(1-7) decreased IL-6 levels in diseased periodontal tissues (Fig. 5). Both the number of IL-6 expressing cells, especially fibroblasts and inflammatory cells (Fig. 5A and D), and IL-6 levels detected by ELISA reduced after Ang-(1-7) therapy (Fig. 5B). DIZE effect was milder. In contrast, IL-1β expression was not affected by Ang-(1-7) or DIZE in periodontal tissues (Fig. 5C). Thus, the observed effects may derive partially from reduction in cytokine release but also from direct action on osteoblast/osteoclast metabolism.

3.5. The ACE2/Ang-(1-7)/MasR axis in human gingival tissue from healthy and periodontitis patients

Given the experimental results, we further evaluated the expression of ACE2 and MasR in human periodontal tissues. Similarly to the experimental setting, gingival samples from healthy donors presented strong immuno-staining for ACE2 (Fig. 6A) and MasR (Fig. 6B). The positive cells were mainly epithelial cells, endothelial cells, fibroblasts, and some mononuclear inflammatory cells. In contrast, immunostaining was significantly weak in samples from patients with periodontitis (Fig. 6). In the inflamed samples, the stained cells were mainly inflammatory cells, especially mononuclear cells and endothelial cells. These results indicate that the ACE2/Ang-(1-7)/MasR axis is downregulated in the dysbiotic and inflammatory periodontal environment associated to alveolar bone resorption.

4. Discussion

The relevance of the RAS as a local hormonal system that may control homeostatic and inflammatory conditions in different tissues has received increasing attention lately. From the classical hormonal events whose description began in 1898 with the discovery of renin [27] to the recent description of new components of this peptidic cascade [2], much has been learned but still has to be characterized. In the current study, we showed the expression of ACE2/MasR by osteoblasts and osteoclasts and demonstrated how the activation of the ACE2/Ang-(1-7)/MasR axis can impact bone turnover *in vitro* and *in vivo*.

Distinct cells and tissues express locally active RAS components [11,28–31]. To the well-known expression of kidney renin and ACE2, lung ACE and hepatic angiotensinogen [32], recent data added RAS components synthesis by several other cells/tissues. This includes heart muscle cells [30] and fibroblasts [31], synovial tissue cells [11,33], gum fibroblasts [34,35] and inflammatory cells [36,37]. Herein, we evidenced the synthesis of ACE2 and MasR by osteoblasts and osteoclasts. Additionally, we showed that cell stimulation with the bacterial virulence factor LPS slightly downregulated ACE2 expression by osteoblasts. These data are in line with previous studies that demonstrated the presence of some RAS components in bone cells [38]. Lamparter et al. (1998) suggested that osteoblasts may express the AT_1R. It is also known that osteossarcoma cells express ACE2 and MasR [28]. Moreover, monocytes/macrophages, which are osteoclast precursors, synthesize AT_1R [36] and MasR [39,40]. Thus, current data moves a step forward in the characterization of RAS components expression by bone cells.

We further evaluated the effects of ACE2/Ang-(1-7)/MasR axis activation *in vitro* and *in vivo*. To that end, we first stimulated cells directly with Ang-(1-7) or indirectly with DIZE, a compound that activates ACE2 and thus favors Ang-(1-7) synthesis [25]. Although the effects of DIZE were milder than those induced by Ang-(1-7), both strategies improved osteoblast activity, which was specially evidenced by increased osteocalcin and collagen 1A mRNA levels, and decreased osteoclast differentiation, as evidenced by reduced RANK and IL-1β mRNA levels. Indeed, Krishnan et al. (2013) detected reduced osteoclastogenesis from bone marrow cells after Ang-(1-7) treatment in a non-inflammatory milieu [19]. *In vivo*, we investigated the effects of ACE2/Ang-(1-7)/MasR axis activation using a classical experimental model of alveolar bone resorption in rats [23,41]. The placement of a thread around the tooth of rats induces dysbiosis, which triggers inflammatory alveolar bone loss. This is the hallmark of periodontitis, the leading cause of tooth loss in developed countries [42,43]. Similarly to *in vitro* conditions, osteoblasts and osteoclasts, and also fibroblasts, epithelial and endothelial cells, were immunostained for ACE2 and MasR in periodontal tissues. Nevertheless, such expression decreased in diseased samples. Accordingly, Santos et al. (2015) found RAS

components mRNA, including ACE2 and MasR, in gingival homogenates of healthy and periodontitis rat samples [34]. ACE2 and MasR were also detected in osteoporotic rat femurs [17,18]. In this setting, local ACE2/Ang-(1-7)/MasR axis activation reduced bone resorption through improvement of osteoblast/osteoclast ratio. Such improved phenotype in a dysbiotic inflammatory condition is similar to the protective effects induced by Ang-(1-7) in experimental osteoporosis, *i.e.* the heptapetide improved bone properties and prevented biochemical alterations triggered by ovarietomy in rats [17,18].

Aside the direct effects of ACE2/Ang-(1-7)/MasR axis activation on bone cells, at least part of the observed protective phenotype could derive from Ang-(1-7) anti-inflammatory properties [44]. Several evidence indicate that Ang-(1-7) can decrease the expression of cytokines directly related to bone resorption, such as IL-1β, IL-6 and TNF, in a wide range of inflammatory conditions [8–11]. Herein, ACE2/Ang-(1-7)/MasR axis activation reduced IL-6 levels *in vitro* and *in vivo*, but had mild effects on IL-1β *in vivo*. Indeed, ACE2 deficient mice express higher levels of IL-6 than wild type mice [45]. In this regard, IL-6 is a pro-osteoclastogenesis cytokine directly involved in alveolar bone resorption associated to dysbiosis [26]. IL-6 favors osteoclast differentiation [46] and, in a dysbiotic inflammatory milieu, it induces the conversion of FoxP3 T cells to Th17 cells, which protect against bacteria but induces bone damage [26]. Thus, the protective bone effects triggered by Ang-(1-7) were at least in part derived from its anti-inflammatory potential.

Ultimately, in line with the experimental evidence of ACE2/Ang-(1-7)/MasR protagonism in bone remodeling, we qualitatively showed that human gingival samples had the same experimental pattern of ACE2 and MasR protein expression in healthy and diseased periodontal tissues. This is in line with a previous study indicating the mRNA presence of ACE2 and MasR in gum homogenates [34]. These data point the potential translation of this pathway to the clinical context. Inflammatory bone resorptive conditions are still a challenge worldwide and, thus, deserve continuous investigation of new paths for intervention.

In conclusion, current data shows that osteoblasts and osteoclasts express ACE2 and MasR and that ACE2/Ang-(1-7)/MasR axis activation reduces the bone resorptive milieu by modulating bone cells phenotype at least in part for its anti-inflammatory properties. Therefore, the ACE2/Ang-(1-7)/MasR is an active player in alveolar bone remodeling.

Supplementary data to this article can be found online at https://doi.org/10.1016/j.bone.2019.115041.

Acknowledgments

This study was financed in part by the Coordenação de Aperfeiçoamento de Pessoal de Nível Superior - Brasil (CAPES) - Finance Code 001; Fundação de Amparo à Pesquisa do Estado de Minas Gerais - FAPEMIG and National Council for Scientific and Technological Development - CNPq.

References

[1] B.J. Hoogwerf, Renin-angiotensin system blockade and cardiovascular and renal protection, Am. J. Cardiol. 105 (2010) 30A–35A, https://doi.org/10.1016/j.amjcard.2009.10.009.

[2] R.Q. Lautner, D.C. Villela, R.A. Fraga-Silva, N. Silva, T. Verano-Braga, F. Costa-Fraga, J. Jankowski, V. Jankowski, F. Sousa, A. Alzamora, E. Soares, C. Barbosa, F. Kjeldsen, A. Oliveira, J. Braga, S. Savergnini, G. Maia, A.B. Peluso, D. Passos-Silva, A. Ferreira, F. Alves, A. Martins, M. Raizada, R. Paula, D. Motta-Santos, F. Kemplin, A. Pimenta, N. Alenina, R. Sinisterra, M. Bader, M.J. Campagnole-Santos, R.A.S. Santos, Discovery and characterization of alamandine: a novel component of the renin-angiotensin system, Circ. Res. 112 (2013) 1104–1111, https://doi.org/10.1161/CIRCRESAHA.113.301077.

[3] M. Bader, Tissue renin-angiotensin-aldosterone systems: targets for pharmacological therapy, Annu. Rev. Pharmacol. Toxicol. 50 (2010) 439–465, https://doi.org/10.1146/annurev.pharmtox.010909.105610.

[4] K.D. Silveira, F.M. Coelho, A.T. Vieira, L.C. Barroso, C.M. Queiroz, V.V. Costa, L.F.C. Sousa, M.L. Oliveira, M. Bader, T.A. Silva, R.A.S. Santos, A.C. Simões, E. Silva, M.M. Teixeira, Mechanisms of the anti-inflammatory actions of the angiotensin type1 receptor antagonist losartan in experimental models of arthritis, Peptides 46 (2013) 53–63, https://doi.org/10.1016/j.peptides.2013.05.012.

[5] J. Wang, L. Chen, B. Chen, A. Meliton, S.Q. Liu, Y. Shi, T. Liu, D.K. Deb, J. Solway, Y. Chun Li, Chronic activation of the renin-angiotensin system induces lung fibrosis, Sci. Rep. 5 (2015) 1–11, https://doi.org/10.1038/srep15561.

[6] S.H. Min, S.H. Kong, J.E. Lee, D.H. Lee, T.J. Oh, K.M. Kim, K.S. Park, H.C. Jang, S. Lim, Association of angiotensin-II levels with albuminuria in subjects with normal glucose metabolism, prediabetes, and type 2 diabetes mellitus, J. Diabetes Complicat. 31 (2017) 1499–1505, https://doi.org/10.1016/j.jdiacomp.2017.07.002.

[7] W.-Y. Hsieh, T.-H. Chang, H.-F. Chang, W.-H. Chuang, L.-C. Lu, C.-W. Yang, C.-S. Lin, C.-C. Chang, Renal chymase-dependent pathway for angiotensin II formation mediated acute kidney injury in a mouse model of aristolochic acid I-induced acute nephropathy, PLoS One 14 (2019) e0210656, , https://doi.org/10.1371/journal.pone.0210656.

[8] M.A. Khajah, M.M. Fateel, K.V. Ananthalakshmi, Y.A. Luqmani, Anti-inflammatory action of angiotensin 1-7 in experimental colitis may be mediated through modulation of serum cytokines/chemokines and immune cell functions, Dev. Comp. Immunol. 74 (2017) 200–208, https://doi.org/10.1016/j.dci.2017.05.005.

[9] W. Lu, J. Kang, K. Hu, S. Tang, X. Zhou, S. Yu, Y. Li, L. Xu, Angiotensin-(1-7) inhibits inflammation and oxidative stress to relieve lung injury induced by chronic intermittent hypoxia in rats, Braz. J. Med. Biol. Res. 49 (2016) 1–9, https://doi.org/10.1590/1414-431X20165431.

[10] A.M. Papinska, M. Soto, C.J. Meeks, K.E. Rodgers, Long-term administration of angiotensin (1-7) prevents heart and lung dysfunction in a mouse model of type 2 diabetes (db/db) by reducing oxidative stress, inflammation and pathological remodeling, Pharmacol. Res. 107 (2016) 372–380, https://doi.org/10.1016/j.phrs.2016.02.026.

[11] K.D. da Silveira, F.M. Coelho, A.T. Vieira, D. Sachs, L.C. Barroso, V.V. Costa, T.L.B. Bretas, M. Bader, L.P. de Sousa, T.A. da Silva, R.A.S. dos Santos, A.C. e S. Simões, M.M. Teixeira, Anti-inflammatory effects of the activation of the angiotensin-(1 − 7) receptor, mas, in experimental models of arthritis, J. Immunol. (2010), https://doi.org/10.4049/jimmunol.1000314.

[12] L.C. Barroso, G.S. Magalhaes, I. Galvão, A.C. Reis, D.G. Souza, L.P. Sousa, R.A.S. Santos, M.J. Campagnole-Santos, V. Pinho, M.M. Teixeira, Angiotensin-(1-7) promotes resolution of neutrophilic inflammation in a model of antigen-induced arthritis in mice, Front. Immunol. 8 (2017), https://doi.org/10.3389/fimmu.2017.01596.

[13] H. Shimizu, H. Nakagami, M.K. Osako, R. Hanayama, Y. Kunugiza, T. Kizawa, T. Tomita, H. Yoshikawa, T. Ogihara, R. Morishita, Angiotensin II accelerates osteoporosis by activating osteoclasts, FASEB J. 22 (2008) 2465–2475, https://doi.org/10.1096/fj.07-098954.

[14] Y. Asaba, M. Ito, T. Fumoto, K. Watanabe, R. Fukuhara, S. Takeshita, Y. Nimura, J. Ishida, A. Fukamizu, K. Ikeda, Activation of renin-angiotensin system induces osteoporosis independently of hypertension, J. Bone Miner. Res. 24 (2009) 241–250, https://doi.org/10.1359/jbmr.081006.

[15] A.P. Moura, C.C. Montalvany-Antonucci, S.R.D.A. Taddei, C.M. Queiroz-Junior, C.C. Biguetti, G.P. Garlet, A.J. Ferreira, M.M. Teixeira, T.A. Silva, I. Andrade, Effects of angiotensin II type I receptor blocker losartan on orthodontic tooth movement, Am. J. Orthod. Dentofac. Orthop. 149 (2016) 358–365, https://doi.org/10.1016/j.ajodo.2015.09.019.

[16] C.M. Queiroz-Junior, K.D. Silveira, C.R. de Oliveira, A.P. Moura, M.F.M. Madeira, F.M. Soriani, A.J. Ferreira, S.Y. Fukada, M.M. Teixeira, D.G. Souza, T.A. da Silva, Protective effects of the angiotensin type 1 receptor antagonist losartan in infection-induced and arthritis-associated alveolar bone loss, J. Periodontal Res. 50 (2015) 814–823, https://doi.org/10.1111/jre.12269.

[17] H.M. Abuohashish, M.M. Ahmed, D. Sabry, M.M. Khattab, S.S. Al-Rejaie, Angiotensin (1-7) ameliorates the structural and biochemical alterations of ovariectomy-induced osteoporosis in rats via activation of ACE-2/Mas receptor axis, Sci. Rep. 7 (2017) 1–11, https://doi.org/10.1038/s41598-017-02570-x.

[18] H.M. Abuohashish, M.M. Ahmed, D. Sabry, M.M. Khattab, S.S. Al-Rejaie, The ACE-2/Ang1-7/Mas cascade enhances bone structure and metabolism following angiotensin-II type 1 receptor blockade, Eur. J. Pharmacol. 807 (2017) 44–55, https://doi.org/10.1016/j.ejphar.2017.04.031.

[19] B. Krishnan, T.L. Smith, P. Dubey, M.E. Zapadka, F.M. Torti, M.C. Willingham, E.A. Tallant, P.E. Gallagher, Angiotensin-(1-7) attenuates metastatic prostate cancer and reduces osteoclastogenesis, Prostate 73 (2013) 71–82, https://doi.org/10.1002/pros.22542.

[20] M.A. Sá, H.J. Ribeiro, T.M. Valverde, B.R. Sousa, P.A. Martins Jünior, R.M. Mendes, L.O. Ladeira, R.R. Resende, G.T. Kitten, A.J. Ferreira, Single-walled carbon nanotubes functionalized with sodium hyaluronate enhance bone mineralization, Braz. J. Med. Biol. Res. 49 (2016) 1–10, https://doi.org/10.1590/1414-431X20154888.

[21] T.M. da M. Martins, A.C.C. de Paula, D.A. Gomes, A.M. Goes, Alkaline phosphatase expression/activity and multilineage differentiation potential are the differences between fibroblasts and orbital fat-derived stem cells – a study in animal serum-free culture conditions thaís, Stem Cell Rev. Rep. 41 (2014) 3156–3162, https://doi.org/10.1007/s12015-014-9529-9.

[22] T.H. Lin, R. Sen Yang, C.H. Tang, M.Y. Wu, W.M. Fu, Regulation of the maturation of osteoblasts and osteoclastogenesis by glutamate, Eur. J. Pharmacol. 589 (2008) 37–44, https://doi.org/10.1016/j.ejphar.2008.04.060.

[23] K. Sallay, F. Sanavi, I. Ring, P. Pham, U.H. Behling, A. Nowotny, Alveolar bone destruction in the immunosuppressed rat, J. Periodontal Res. 17 (1982) 263–274, https://doi.org/10.1111/j.1600-0765.1982.tb01153.x.

[24] C.M. Queiroz-Junior, K.L.M. Maltos, D.F. Pacheco, T.A. Silva, J.D.S. Albergaria, C.M.F. Pacheco, Endogenous opioids regulate alveolar bone loss in a periodontal

disease model, Life Sci. 93 (2013) 471–477, https://doi.org/10.1016/j.lfs.2013.08.007.
[25] J.A. Hernández Prada, A.J. Ferreira, M.J. Katovich, V. Shenoy, Y. Qi, R.A.S. Santos, R.K. Castellano, A.J. Lampkins, V. Gubala, D.A. Ostrov, M.K. Raizada, Structure-based identification of small-molecule angiotensin-converting enzyme 2 activators as novel antihypertensive agents, Hypertension 51 (2008) 1312–1317, https://doi.org/10.1161/HYPERTENSIONAHA.107.108944.
[26] M. Tsukasaki, N. Komatsu, K. Nagashima, T. Nitta, W. Pluemsakunthai, C. Shukunami, Y. Iwakura, T. Nakashima, K. Okamoto, H. Takayanagi, Host defense against oral microbiota by bone-damaging T cells, Nat. Commun. 9 (2018) 1–11, https://doi.org/10.1038/s41467-018-03147-6.
[27] N. Basso, N. Terragno A, History about the discovery of the renin-angiotensin system, vol. 73, (2001), pp. 720–730, https://doi.org/10.1002/ajp.20949.Social.
[28] S.A. Ender, A. Dallmer, F. Lässig, U. Lendeckel, C. Wolke, Expression and function of the ACE2/angiotensin(1-7)/Mas axis in osteosarcoma cell lines U-2 OS and MNNG-HOS, Mol. Med. Rep. 10 (2014) 804–810, https://doi.org/10.3892/mmr.2014.2266.
[29] W. Asghar, A. Aghazadeh-Habashi, F. Jamali, Cardiovascular effect of inflammation and nonsteroidal anti-inflammatory drugs on renin–angiotensin system in experimental arthritis, Inflammopharmacology 25 (2017) 543–553, https://doi.org/10.1007/s10787-017-0344-1.
[30] R. Kumar, V.P. Singh, K.M. Baker, The intracellular renin-angiotensin system in the heart c, Curr. Hypertens. Rep. 11 (2019) 104–110 https://www.ncbi.nlm.nih.gov/pubmed/19278599.
[31] A. Tadevosyan, J. Xiao, S. Surinkaew, P. Naud, C. Merlen, M. Harada, X. Qi, D. Chatenet, A. Fournier, B.G. Allen, S. Nattel, Intracellular angiotensin-II interacts with nuclear angiotensin receptors in cardiac fibroblasts and regulates RNA synthesis, cell proliferation, and collagen secretion, J. Am. Heart Assoc. 6 (2017), https://doi.org/10.1161/JAHA.116.004965.
[32] R.M. Carey, H.M. Siragy, Newly recognized components of the renin-angiotensin system: potential roles in cardiovascular and renal regulation, Endocr. Rev. 24 (2003) 261–271, https://doi.org/10.1210/er.2003-0001.
[33] A. Price, J.C. Lockhart, W.R. Ferrell, W. Gsell, S. McLean, R.D. Sturrock, Angiotensin II type 1 receptor as a novel therapeutic target in rheumatoid arthritis: in vivo analyses in rodent models of arthritis and ex vivo analyses in human inflammatory synovitis, Arthritis Rheum. 56 (2007) 441–447, https://doi.org/10.1002/art.22335.
[34] C.F. Santos, A.C. Morandini, T.J. Dionísio, F.A. Faria, M.C. Lima, C.M. Figueiredo, B.L. Colombini-Ishikiriama, C.R. Sipert, R.P. Maciel, A.P. Akashi, G.P. Souza, G.P. Garlet, C.O. Rodini, S.L. Amaral, C. Becari, M.C. Salgado, E.B. Oliveira, I. Matus, D.N. Didier, A.S. Greene, Functional local renin-angiotensin system in human and rat periodontal tissue, PLoS One 10 (2015) 1–26, https://doi.org/10.1371/journal.pone.0134601.
[35] C.F. Santos, A.E. Akashi, T.J. Dionísio, C.R. Sipert, D.N. Didier, A.S. Greene, S.H.P. Oliveira, H.J.V. Pereira, C. Becari, E.B. Oliveira, M.C.O. Salgado, Characterization of a local renin-angiotensin system in rat gingival tissue, J. Periodontol. 80 (2009) 130–139, https://doi.org/10.1902/jop.2009.080264.
[36] A. Okamura, H. Rakugi, M. Ohishi, Y. Yanagitani, S. Takiuchi, K. Moriguchi, P.A. Fennessy, J. Higaki, T. Ogihara, Upregulation of renin-angiotensin system during differentiation of monocytes to macrophages, J. Hypertens. 17 (1999) 537–545, https://doi.org/10.1097/00004872-199917040-00012.
[37] C. Owen, E.J. Campbell, Angiotensin II generation at the cell surface of activated neutrophils: novel cathepsin G-mediated catalytic activity that is resistant to inhibition, J. Immunol. 160 (1998) 1436–1443 http://www.ncbi.nlm.nih.gov/pubmed/9570564.
[38] S. Lamparter, L. Kling, M. Schrader, R. Ziegler, J. Pfeilschifter, Effects of angiotensin II on bone cells in vitro, J. Cell. Physiol. 175 (1998) 89–98, https://doi.org/10.1002/(SICI)1097-4652(199804)175:1<89::AID-JCP10>3.0.CO;2-J.
[39] A. Hammer, G. Yang, J. Friedrich, A. Kovacs, D.-H. Lee, K. Grave, S. Jörg, N. Alenina, J. Grosch, J. Winkler, R. Gold, M. Bader, A. Manzel, L.C. Rump, D.N. Müller, R.A. Linker, J. Stegbauer, Role of the receptor Mas in macrophage-mediated inflammation in vivo, Proc. Natl. Acad. Sci. 113 (2016) 14109–14114, https://doi.org/10.1073/pnas.1612668113.
[40] L.L. Souza, C.M. Costa-Neto, Angiotensin-(1-7) decreases LPS-induced inflammatory response in macrophages, J. Cell. Physiol. 227 (2012) 2117–2122, https://doi.org/10.1002/jcp.22940.
[41] C.M. Queiroz-Junior, C.M.F. Pacheco, K.L.M. Maltos, M.V. Caliari, I.D.G. Duarte, J.N. Francischi, Role of systemic and local administration of selective inhibitors of cyclo-oxygenase 1 and 2 in an experimental model of periodontal disease in rats, J. Periodontal Res. 44 (2009) 153–160, https://doi.org/10.1111/j.1600-0765.2007.01069.x.
[42] P.I. Eke, L. Wei, W.S. Borgnakke, G. Thornton-Evans, X. Zhang, H. Lu, L.C. McGuire, R.J. Genco, Periodontitis prevalence in adults ≥65 years of age, in the USA, Periodontol 2000 (72) (2016) 76–95, https://doi.org/10.1111/prd.12145.
[43] J. Marchesan, M.S. Girnary, L. Jing, M.Z. Miao, S. Zhang, L. Sun, T. Morelli, M.H. Schoenfisch, N. Inohara, S. Offenbacher, Y. Jiao, An experimental murine model to study periodontitis, Nat. Protoc. 13 (2018) 2247–2267, https://doi.org/10.1038/s41596-018-0035-4.
[44] T.R. Rodrigues Prestes, N.P. Rocha, A.S. Miranda, A.L. Teixeira, A.C. Simoes-e-Silva, The anti-inflammatory potential of ACE2/angiotensin-(1-7)/Mas Receptor Axis: evidence from basic and clinical research, Curr. Drug Targets 18 (2017) 1301–1313, https://doi.org/10.2174/1389450117666160727142401.
[45] M.C. Thomas, R.J. Pickering, D. Tsorotes, A. Koitka, K. Sheehy, S. Bernardi, B. Toffoli, T.P. Nguyen-Huu, G.A. Head, Y. Fu, J. Chin-Dusting, M.E. Cooper, C. Tikellis, Genetic Ace2 deficiency accentuates vascular inflammation and atherosclerosis in the ApoE knockout mouse, Circ. Res. 107 (2010) 888–897, https://doi.org/10.1161/CIRCRESAHA.110.219279.
[46] K. Yokota, K. Sato, T. Miyazaki, H. Kitaura, H. Kayama, F. Miyoshi, Y. Araki, Y. Akiyama, K. Takeda, T. Mimura, Combination of tumor necrosis factor α and interleukin-6 induces mouse osteoclast-like cells with bone resorption activity both in vitro and in vivo, Arthritis Rheum. 66 (2014) 121–129, https://doi.org/10.1002/art.38218.